Results in Chemistry 17 (2025) 102573



Contents lists available at ScienceDirect

Results in Chemistry

journal homepage: www.sciencedirect.com/journal/results-in-chemistry





Potential for optimisation of fuel yield and hydrocarbon distribution from plastic waste pyrolysis using Nanopyroxene catalysts

Derick Muloogi [a,*], Farad Sagala [a], Fortunate Ogene [a], Denis Bbosa [b], Grace Birungi [c]

[a] Department of Energy, Minerals and Petroleum Studies, Mbarara University of Science and Technology, P. O. Box 1410 Mbarara, Uganda
[b] Department of Mechanical and Industrial Engineering, Mbarara University of Science and Technology, P. O. Box 1410 Mbarara, Uganda
[c] Department of Chemistry, Mbarara University of Science and Technology, P. O. Box 1410 Mbarara, Uganda

ARTICLE INFO

Keywords:
Nanopyroxene
Plastic waste
Thermal pyrolysis
Physico-chemical characteristics
Gas chromatography-mass spectrometer

ABSTRACT

Plastic waste is a global concern, driven largely by the widespread use of single-use plastics. Despite advances in recycling technologies, scalable, and cost-effective plastic waste management solutions remain limited. Thermal pyrolysis offers a complementary pathway for plastic waste valorisation through energy recovery, but conventional processes are constrained by slow reaction rates, high energy demands, and low fuel yields. This study introduces, for the first time, nanopyroxene as a novel catalytic additive for plastic waste pyrolysis in a locally fabricated batch reactor, aiming to improve fuel yield and hydrocarbon distribution. A mixture of Low-density polyethylene (LDPE), High-density polyethylene (HDPE), and polypropylene (PP) (2:1:2 ratio) was thermally decomposed under catalysed and non-catalysed conditions. The physico-chemical properties of the resulting plastic-derived fuel oils (PDFOs) were benchmarked against commercial diesel. Catalytic pyrolysis significantly increased the fuel oil yield to 77 %, compared to 56 % from non-catalytic pyrolysis ($p < 0.05$). The catalyst promoted the formation of light hydrocarbons (C_1–C_9) and reduced intermediate fractions but increased ultra-heavy hydrocarbons (C_{25}–C_{56}), which potentially affects combustion efficiency. Physical characterisation revealed no statistically significant differences ($p > 0.05$) between PDFOs and commercial diesel in key fuel properties, all of which fell within recommended standards. However, PDFOs exhibited higher volatility, density, and flammability, with lower flash and fire points (39 °C, 48 °C), suggesting suitability for high-energy combustion applications. These findings demonstrate the potential of nanopyroxene to enhance fuel yield and quality from plastic pyrolysis, though further optimisation, detailed catalytic mechanisms, and comprehensive environmental impact assessments are necessary for large-scale adoption.

1. Introduction

Plastics are deeply embedded in our daily lives, with approximately 50 % used for single-use items like packaging and disposable products, 20–25 % for long-lasting infrastructure such as pipes and cable coatings, and the rest in durable consumer goods like electronics, furniture, and vehicles [1,2,3]. As plastic waste continues to rise, preserving the environment demands more efficient and cost-effective waste management strategies. However, traditional methods like landfills and incineration often exacerbate environmental harm. For example, incineration releases harmful greenhouse gases like CO_2 [4], while landfills can lead to toxic percolation into groundwater [5,6,7], underpinning the need for reliable, scalable, and eco-friendly alternatives.

With millions of tons of plastic waste generated worldwide [8], only 9 % is recycled [9], a value significantly lower than the earlier estimate of 12 % [10]. In Uganda, the production of plastic waste is steadily increasing, with an estimated 600 metric tons generated daily [11]. This growing plastic waste problem, alongside the inadequate waste management infrastructure in many low-income countries, including Uganda, amplifies the challenges of plastic disposal and management. If left unaddressed, plastic accumulation could lead to severe environmental consequences, including soil degradation, clogged waterways, and urban flooding [12,13]. These impacts threaten the survival of various species and the stability of ecosystems. As a result, recycling has become a crucial measure to address these impacts, evolving into one of the most dynamic sectors in the plastics industry today [10].

The most commonly used recycling technique is mechanical recycling [10]; [14], but faces limitations with heterogeneous and

* Corresponding author.
E-mail address: dmuloogi@must.ac.ug (D. Muloogi).

https://doi.org/10.1016/j.rechem.2025.102573
Received 12 May 2025; Accepted 28 July 2025
Available online 5 August 2025
2211-7156/© 2025 The Authors. Published by Elsevier B.V. This is an open access article under the CC BY license (http://creativecommons.org/licenses/by/4.0/).

contaminated plastics. Advanced valorisation strategies, such as producing biochar-reinforced composites, have shown promise in improving the mechanical and thermal properties of recycled polymers, reflecting efforts to maximise plastic waste within a circular economy [15,16]. However, in low-income settings like Uganda, where the requisite material- processing infrastructure is limited and energy scarcity is still a critical challenge, material recovery alone may not offer an immediate solution. Energy recovery through pyrolysis presents a more practical and locally adaptable pathway, converting plastic waste into diesel-like fuels while directly addressing both waste accumulation and localised energy demand [17,18,19].

Among energy recovery approaches, thermal pyrolysis has attracted particular interest for its ability to convert diverse plastic wastes into valuable hydrocarbon fuels under controlled conditions [20,21,17,22]. Typically conducted at temperatures between 450 and 800 °C, thermal pyrolysis produces a carbonised char and a volatile fraction. The volatile fraction can be further separated into condensable hydrocarbon oil and non-condensable gas, which have high calorific values [23]. The quality and composition of the resulting fractions are highly dependent on the nature of the primary feedstock and reaction conditions, such as temperature, pressure, and/or the use of additives. However, conventional thermal pyrolysis remains a slow, energy-intensive process that often results in low yields of usable products [24]. Moreover, the resulting fuels may contain unsaturated hydrocarbons that contribute to environmentally hazardous emissions such NO_X and carbon monoxide [17], although, blending with additives like ethanol can improve combustion efficiency and reduce emissions [18]. Nonetheless, from an operational standpoint, the cost structure of pyrolysis plants and their return on investment remain misaligned, making the prospects of economic viability challenging [25,26]. These limitations have driven the integration of catalysts to enhance yield, improve efficiency and reduce energy consumption.

Previous studies have demonstrated the potential of catalytic thermal pyrolysis for converting plastic waste into diesel-like fuels with improved efficiency and fuel properties. For example Ni − Mo/laponite catalysts have successfully been used to produce high-quality hydroprocessed pyrolysis oil from polypropylene [17,27]. A variety of other catalysts, such as HZSM-5, FCC [28,29], natural zeolite ([30,31], 2018; [32,33,34]), Red Mud [32], metal oxides [35,36], and heterogeneous Ziegler–Natta catalysts [37,38,39] have been explored. These catalytic processes typically produce low-carbon-chain hydrocarbons, including gasoline-range products, which yield better results than thermal pyrolysis ([24]). Whilst zeolites offer high selectivity for light hydrocarbons, their high cost and tendency to deactivate are significant challenges [40]. Silica-alumina [39] and mesoporous catalysts offer a balance of performance, and clays provide a more economical alternative [41]. Despite these advancements, catalytic additives still face limitations in yield, quality, and recovery efficiency [42], with catalytic pyrolysis using catalysts like HZSM-5 producing only modest liquid yields, and the quality of the resulting oils remaining suboptimal [43].

In recent years, nanoparticles have attracted scientific attention as potential catalysts in pyrolysis [44], owing to their remarkable properties, including a high specific surface area, quantum size effects, and unique nanocrystal shapes [35,36]. The use of nanoparticles has been found to increase the contact area between the catalyst's active material and the surrounding gas or liquid phase, thereby enhancing the reaction efficiency [45]. Among these, nanopyroxene, which is a synthetic analogue of naturally occurring pyroxene minerals, shows promising catalytic potential. Structurally composed of iron-silicate chains with exchangeable sodium ions and hydroxylated surfaces, nanopyroxene exhibits hydrophilic properties, negative surface charge, and strong ion-exchange capabilities [46,47]. These properties can be further enhanced by surface modification, allowing for tailored catalytic activity under hydrothermal conditions [46].While previously applied in enhanced oil recovery and residue asphaltenes breakdown [48,46], its catalytic role in plastic pyrolysis remains unexplored.

To address this knowledge gap, this study investigated, for the first time, the catalytic potential of nanopyroxene in the pyrolysis of Low-Density Polyethylene (LDPE), High-Density Polyethylene (HDPE), and Polypropylene (PP) plastic wastes, using a locally fabricated thermal pyrolysis reactor. Specifically, the study aimed to: (i) compare the yield and composition of Plastic-Derived Fuel Oils (PDFOs) produced with and without nanopyroxene catalysis; (ii) analyse the hydrocarbon distribution of the resulting oils; and (iii) evaluate the physico-chemical properties of PDFOs relative to those of commercially available transportation diesel in Uganda, to assess their suitability as alternative fuels, especially in resource-constrained settings.

2. Methodology

2.1. Materials

Dichloromethane (DCM), with high purity (>99.8 % *v*/v; Sigma-Aldrich); A reactor made out of welded stainless steel; Water, Drums, Detergent Drying mesh; Condenser made out of brass; LPG Gas burner; Stainless pipes; collecting jar; A gas chromatograph interfaced with an Agilent Technologies 5975C mass spectrometer and triple-axis detector; TVOC sensor (Resolution range: 0 to 50/0.01 ppm; Dimensions: 210 L × 60 W × 25 mm D (8.3 × 2.4 × 1.0″). The catalysts used for these experiments were structurally modified nanopyroxene.

2.2. Sample collection

The feedstock used for this study were three different types of plastic wastes i.e., HDPE, LDPE, and PP. These wastes were collected from areas of Kihumuro campus and Mile Three in Mbarara city with the aid of research assistants (cf. Fig. 1). These were packed in sacks and then transported to Kihumuro at the Faculty of Applied Sciences and Technology (FAST) labs where the experiments were carried out.

The commercial oil, a diesel-type transportation fuel, was purchased from a petrol station in Wandegeya, Kampala (Fig. 1). It was included in the study for comparison to evaluate how plastic-derived oils compare with refined fuel stock and to determine their potential suitability for use in diesel engines.

2.3. Nanopyroxene synthesis and characterisation

2.3.1. Nanopyroxene synthesis

Nanopyroxene particles used in this study were synthesised following the protocol that has been reported elsewhere [49,50]. The synthesis followed a hydrothermal approach using a pretreated gel, which was formed through the reaction of separately prepared acidic and basic solutions. The acidic solution was obtained by dissolving 15.021 g of anhydrous $FeCl_3$ hexahydrate in a diluted sulfuric acid solution (prepared by mixing 18.067 g of concentrated H_2SO_4 with 90 g of deionized water) under continuous magnetic stirring at 300 rpm. The basic solution was prepared by dissolving 60.129 g of sodium silicate in a diluted NaOH solution (22.495 g of NaOH in 60 g of deionized water). These solutions were gradually combined over a 10-min period, forming a yellow gel. The resulting gel was then transferred into a 300 mL PARR reactor and subjected to hydrothermal crystallization at 160 °C for 72 h while being agitated at 300 rpm. Following the reaction, the crystallized nanoparticles were separated by filtration and rinsed with deionized water until the pH approached neutrality. A schematic representation of the synthesis procedure is provided in Fig. 2. The recovered solid was subsequently dried overnight at 25 °C, yielding nanopyroxene.

2.3.2. Nanopyroxene characterisation

The morphology and surface topology of the sample were characterised using a JEM-2100 scanning electron microscope (SEM) from JEOL Ltd., following the methods detailed elsewhere [51]. A small quantity of each powder was mounted on a carbon tape affixed to a

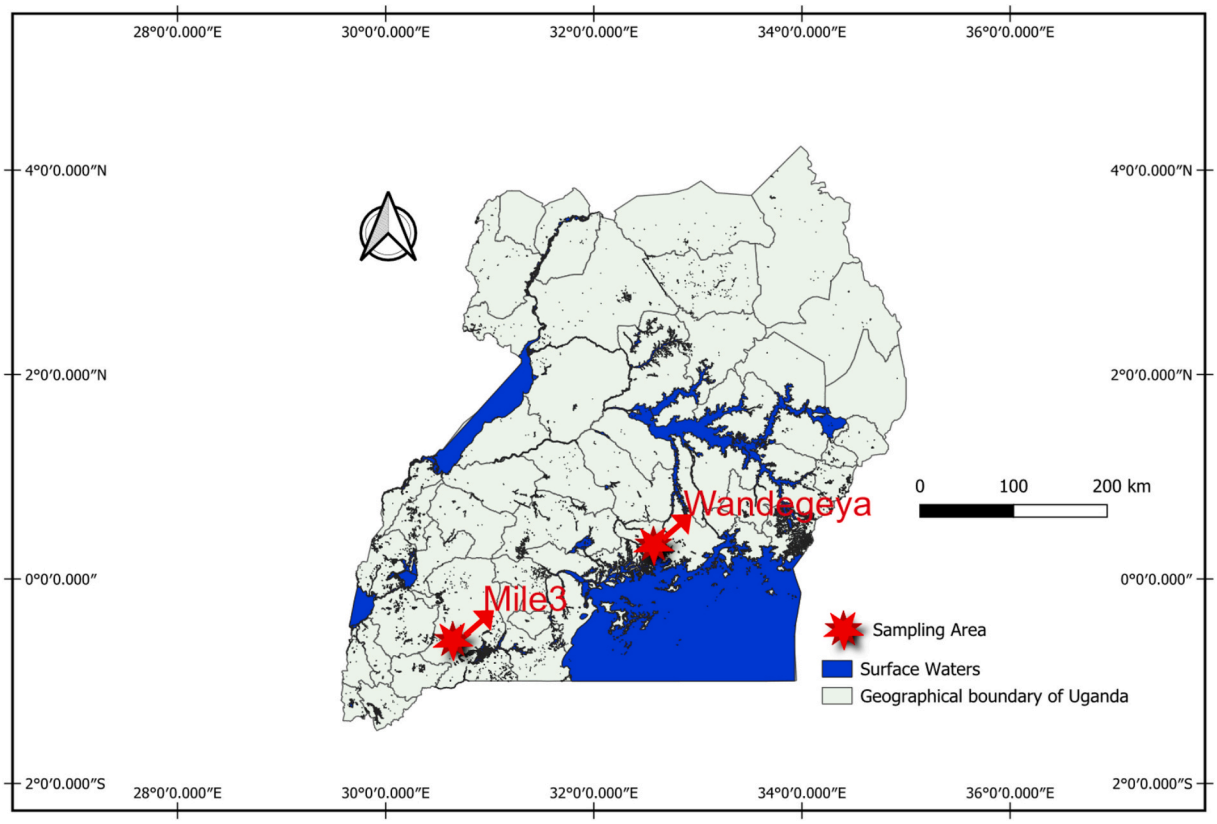


Fig. 1. Map showing the locations of the two sampling sites in Uganda: Mile 3 in Mbarara City where plastic waste was collected, and Wandegeya in Kampala, where diesel oil samples were collected.

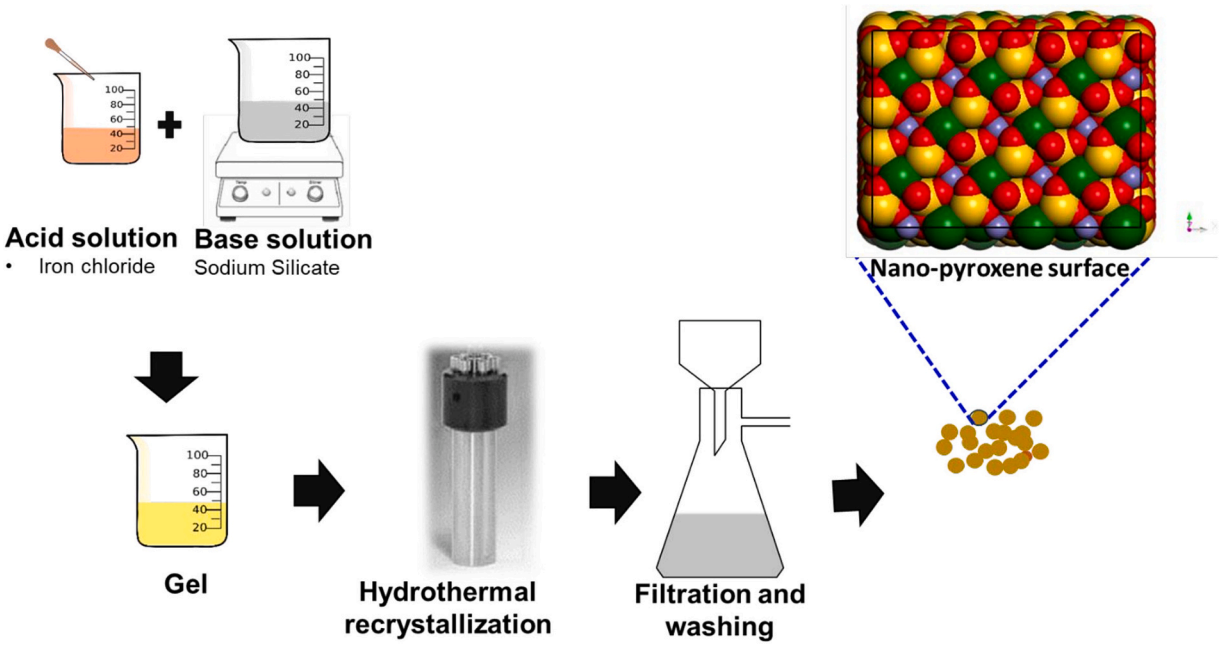


Fig. 2. Schematic representation of the hydrothermal synthesis process of the nanopyroxene nanoparticles, as adopted from Sagala et al., [50]. The process involves gel formation from acidic and basic precursors, followed by hydrothermal crystallization, filtration, and drying to yield nanocrystalline pyroxene with an aegirine structure.

sample holder, and excess material was removed by gently tapping the holder.

High-resolution transmission electron microscopy (TEM) was conducted to further examine particle structure. For this, 0.5 mg of the sample was dispersed in approximately 4 mL of ethanol and sonicated to achieve uniform suspension. A few drops of the dispersion were then deposited onto a Formvar/carbon-coated copper grid and left to dry. Imaging was performed using an FEI Tecnai F20 field emission gun TEM

(FEG-TEM) operated at 200 kV.

X-ray diffraction (XRD) analysis was carried out using a Rigaku ULTIMA III diffractometer equipped with CuKα radiation. Scans were performed over a 2θ range of 3°–90° with a step size of 0.05° and a counting rate of 1.0°/min, operating at 40 kV and 44 mA. Diffraction data were processed using PDXL software (Rigaku), and crystallite sizes were estimated via the Scherrer equation as implemented in the software. Phase identification was conducted by matching the obtained patterns with entries in the Crystallographic Open Database (COD).

2.4. Experimental setup

2.4.1. Reactor fabrication

A locally built, laboratory-scale, externally heated pyrolysis reactor was designed and fabricated to decompose plastics, following the recommendations of Joshi & Seay [52]. Fig. 3 illustrates the schematic representation of the plastic pyrolysis setup used in this study. The key components of the pyrolysis system include a temperature regulator, condenser, heat source, shell gas tank, insulator, and gas exit line. The reactor, made of stainless steel, had an effective length of 480 mm and a diameter of 150 mm.

2.4.2. Thermal and catalytic pyrolysis

Thermal and catalytic pyrolysis was conducted broadly following the methodology outlined by Owusu et al. [22]. A plastic mixture feed of 500 g, with a ratio of 2:1:2 (LDPE: HDPE: PP), was used in the experiment. The plastic wastes were washed using clean water and soap, rinsed with clean distilled water and then dried under the sun. The plastics were then shredded into pieces using a fabricated shredder to generate pieces that were small enough to fit into the reactor through the inlet. The pyrolysis reactor was then ignited to supply the energy needed for the process. The temperature was gradually increased until it reached a range of 330 °C–350 °C, which was maintained for approximately one hour. Subsequently, the temperature was raised to around 450 °C and held until the process was complete. This controlled temperature progression was crucial, as a rapid increase or exceeding 450 °C could result in excessive wax production, while temperatures below 300 °C would cause incomplete feedstock melting, leading to higher char residue in the reactor [53,52]. The recordings of the volume of liquid produced were noted in time intervals of 20 min for 2 h after the first drop. The experiment ran for about 120 min until the reaction was complete. During the process, the waste plastics melted and cracked, releasing hot pyrolysis vapours. These vapours travelled through distillation pipes and were collected in a 5-L container, immersed in water, and the non-condensed gases were flared to the atmosphere. The solid residue (char) was also collected from the reactor after completion of the pyrolysis cycle.

The pyrolysis process was first conducted without a catalyst, followed by a second run using nanopyroxene powder as a catalyst, mixed with the plastic waste at a polymer-to-catalyst ratio of 10:1, as recommended by Owusu et al. [22]. The mass of the resulting liquid fuel (m) was recorded at the end of each experiment. Each experiment was performed in duplicate, with results varying by no more than ±5 %. Fuel oil yield was estimated based on mass, and total conversion percentage was calculated using Eq. (1).

$$Percentage\ yield = \frac{m}{M} \times 100\% \quad (1)$$

where m- is mass of the liquid product in grams.

M- Mass of sample feed in grams.

2.5. Characterisation of plastic derived fuel oil

The physical properties of the fuel oils, including flash point, density, fire point, American Petroleum Institute (API) gravity, specific gravity, smoke point, and flammability, were determined according to the American Society for Testing and Materials (ASTM) standard test methods [54]. These methods ensure consistency and reliability in the evaluation of fuel characteristics. Density and API gravity were tested using ASTM D4052, flash point using ASTM D56, fire point using ASTM D92, smoke point using ASTM D1322, and flammability was inferred based on the flash and fire points [54].

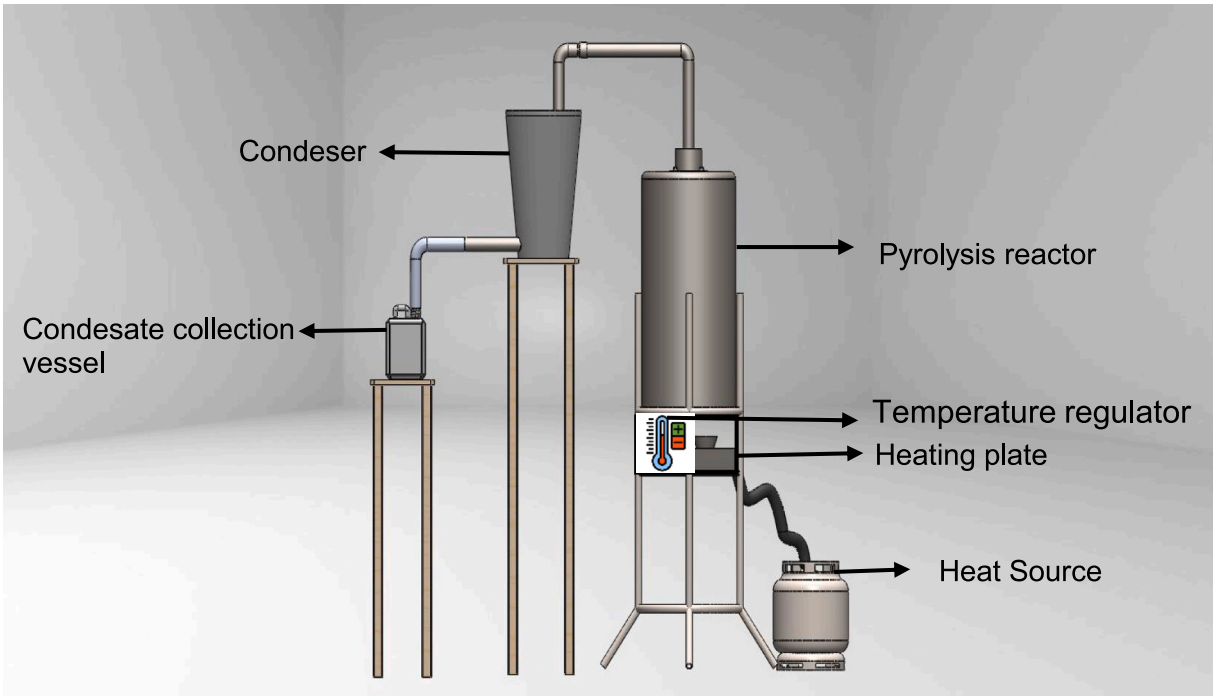


Fig. 3. Annotated schematic representation of the experimental pyrolysis setup for plastic decomposition. The system consists of key components, including a stainless-steel reactor (480 mm length, 150 mm diameter), external heat source, temperature regulator, condenser, gas tank, insulator, and gas exit line. The setup was designed following Joshi & Seay [52] and was used for both thermal and catalytic pyrolysis experiments.

The Total Volatile Organic Compounds (TVOCs) released into the environment during fuel oil combustion were analysed using a TVOC sensor (resolution range: 0–50 ppm; resolution: 0.01 ppm; dimensions: 210 L × 60 W × 25 mm (8.3 × 2.4 × 1.0″)). The inclusion of TVOC analysis provides a quantitative measure of volatile organic compound emissions, which are contributors to air pollution and associated health risks.

2.6. GC/MS analysis of condensable products

The chemical composition of the oils was assessed using the gas chromatography/mass spectrometry (GC–MS) technique. The GC–MS analyses were conducted with an Agilent Technologies 7890 A gas chromatograph interfaced with an Agilent Technologies 5975C mass spectrometer equipped with a triple-axis detector.

Sample preparation involved taking 500 µL of each oil sample, diluting it to 2.5 mL with dichloromethane, and briefly sonicating the mixture. The injection volume for each sample was 5 µL. Analytes were separated using a capillary column (Agilent Technologies HP-5MS, 30 m × 0.25 mm i.d., film thickness: 0.25 µm; Santa Clara, CA, USA) with ultra-high purity helium gas (>99.999 %) as the mobile phase.

The initial oven temperature was set at 60 °C, ramped to 200 °C at a rate of 10 °C/min, and then further ramped at 5 °C/min to 280 °C. The mass source, quadrupole, and injector temperatures were maintained at 230 °C, 150 °C, and 300 °C, respectively. The most abundant signals in each spectrum were identified by comparing the fragmentation patterns from the mass spectra to the National Institute of Standards and Technology (NIST) library.

2.7. Data analysis and processing

Data processing and statistical analyses were performed using R (version 4.4.0) in RStudio (2024.04.0 + 735). All statistical tests were conducted at a 95 % confidence level (α = 0.05). Graphics, where applicable, were generated using both R and OriginPro 2023. Mapping was conducted using QGIS (version 3.36.2-Maidenhead).

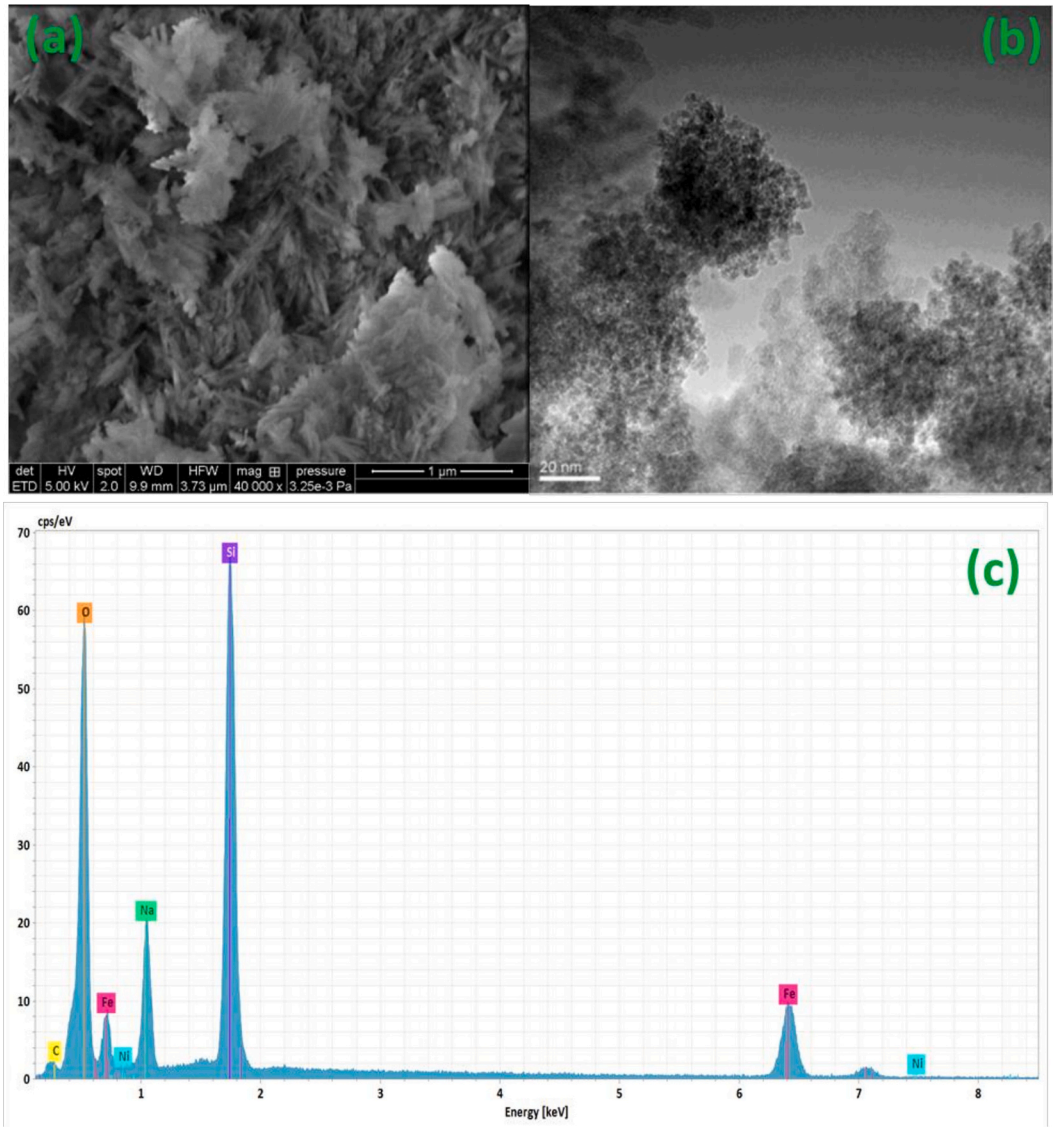


Fig. 4. Characterisation of nanopyroxene using various techniques: **(a)** Scanning Electron Microscope (SEM) revealing uniform morphology and well-defined particle structure; **(b)** High resolution transmission electron microscopy (HRTEM) providing detailed lattice imaging; and **(c)** Energy-Dispersive X-ray Spectroscopy (EDX) confirming the elemental composition of the particles, primarily silicon (Si), iron (Fe), and oxygen (O), consistent with aegirine ($NaFeSi_2O_6$).

3. Results and discussion

3.1. Nanopyroxene characterisation

The characterisation of the nanoparticles was consistent with results previously reported [50]. X-ray diffraction (XRD) analysis indicated a crystalline size of approximately 10 nm, while Brunauer–Emmett–Teller (BET) analysis revealed a surface area of 178.0 m^2/g.

3.1.1. HRTEM, SEM and EDX mapping

SEM imaging (Fig. 4**a**) revealed the well-defined structural integrity of the nanopyroxene particles, showing a uniform morphology. HRTEM (Fig. 4**b**) provides high-resolution images, highlighting the fine structural details of the material. EDX mapping (Fig. 4**c**) was used to verify the elemental composition, showing that the nanopyroxene is primarily composed of silica (Si), iron (Fe), and oxygen (O), which are consistent with the expected composition of aegirine ($NaFeSi_2O_6$) [49].The EDX results across multiple surface points confirm the uniform distribution of these elements, further supporting the structural and chemical integrity of the nanopyroxene.

3.1.2. X-ray diffraction (XRD) patterns of the synthesised nanopyroxene

Fig. 5 shows the X-ray diffraction (XRD) patterns of the synthesised nanopyroxene, confirming the successful formation of the aegirine structure. The obtained diffraction patterns closely match the standard profile from the diffraction file (PDF) card #01–076-2564, as referenced from the 2005 International Centre for Diffraction Data (ICDD). XRD analysis was performed using the JADE V. 7.5.1 software for pattern processing, identification, and quantification.

The hkl and 2θ values, derived from the Crystallographic Open Database (COD) file 9,000,327, indicate that the nanopyroxene crystallises in the C12/c1(15) space group. The unit cell parameters were determined as a = 9.6580 Å, b = 8.7950 Å, c = 5.2940 Å, α = 90.000°, β = 107.420°, γ = 90.000°, and the unit cell volume was calculated to be 429.059 $Å^3$, with Z = 1. These structural parameters are consistent with the characteristics of aegirine, confirming the formation of nanopyroxene with small crystalline domain sizes [46] [47] [50].

3.2. Fuel yield

The mass balance yields of the experimental runs for mixed plastic (LDPE, HDPE and PP) pyrolysis were determined in both the absence and presence of a catalyst. The results (Fig. 6**)** show that in the absence of the catalyst, the percentage yield was at 56 %, while in the presence of the catalyst, the yield was at 77 %.

3.3. Comparison of physical characteristics of plastic-derived fuel oils in the presence of catalyst with commercial oils

Comparing the Plastic-Derived Fuel Oil (PDFO) in presence of a catalyst with Commercial Oil (X) shows a range of differences in their physical properties (Table 1), although these differences were found not to be statistically significant ($p > 0.05$).

Generally, PDFOs are more volatile and flammable than commercial oils, but PDFO's properties also suggest potential for specific industrial applications with proper precautions. PDFO exhibited higher density (863.75 kg/m^3), and specific gravity (0.86) compared to Commercial Oil (835 kg/m^3 and 0.85, respectively). This higher density, likely due to a greater proportion of longer-chain hydrocarbons [19], makes PDFO suitable for applications requiring higher energy content per unit volume, such as certain combustion engines [55], energy-intensive industrial processes, or petrochemical feedstock [56]. However, its higher density may pose challenges in refining, limiting its use in industries reliant on lighter oils [57]. These findings align with Khan et al. [58], who reported Waste Plastic Pyrolysis Oil densities of 747.7–794.3 kg/m^3, and are comparable to the EN 590 standard (820–845 kg/m^3 at 15 °C) **(CEN, 2009)** [59]**.**

Another key difference between the two oils lies in their flashpoint and fire point. PDFO has a lower flashpoint (39 °C), and fire point (48 °C) compared to Commercial Oil (50 °C and 56 °C, respectively), making it more prone to ignition at lower temperatures. Whilst this poses safety risks in handling and storage, it may be advantageous in industries requiring quick combustion or high volatility for efficient fuel use. However, its low flashpoint makes PDFO less suitable for applications prioritising safety and temperature stability. Notably, PDFO's fire point is higher than that reported for waste plastic pyrolysis oil (20 °C) by Khan et al. [58], which could be attributed to the nature of feedstock.

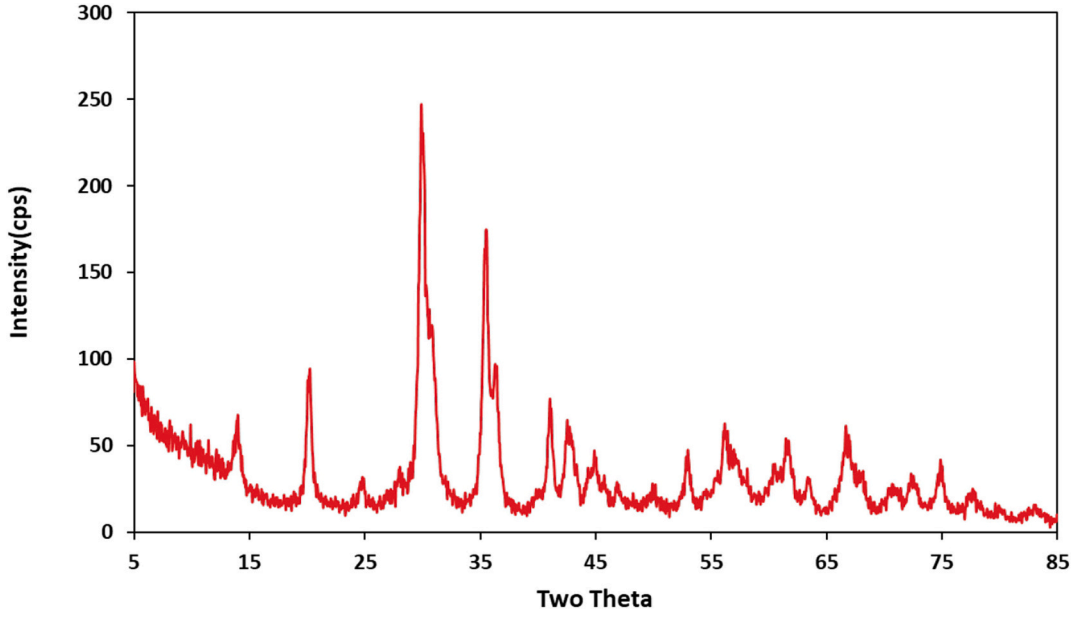


Fig. 5. X-ray diffraction (XRD) pattern for the synthesised nanopyroxene, confirming formation of the aegirine phase. The peaks match the standard aegirine pattern (PDF card #01–076-2564, COD file 9,000,327), consistent with the C12/c1(15) space group and unit cell parameters a = 9.6580 Å, b = 8.7950 Å, c = 5.2940 Å, β = 107.420°.

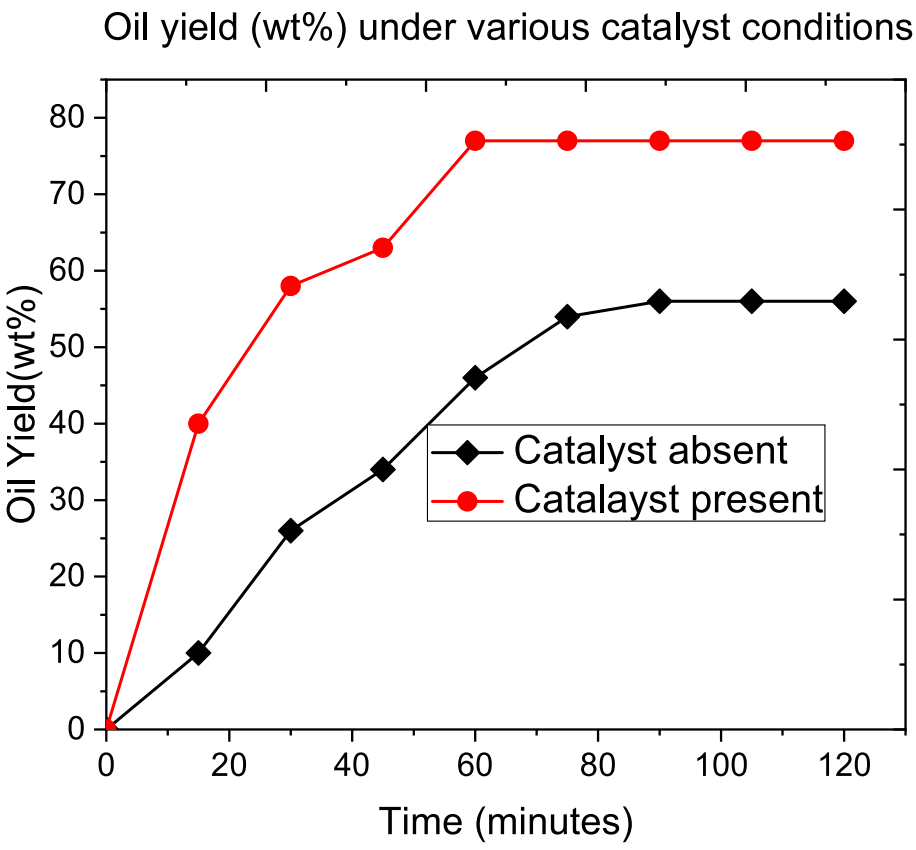


Fig. 6. Relationship between the percentage oil yield in the presence and absence of catalyst with reaction time. The yield was calculated by dividing the mass of the oil produced by the mass of plastic feedstock used.

Table 1
Properties of PDFOs in presence of catalyst and commercial transportation diesel oil.

Property (Units)	Plastic Derived Oil in Presence of Catalyst	Commercial Oil
Density (kg/ m^3)	863.75	835
API Gravity (^{0}API)	32.46	34.97
Flashpoint (^{0}c)	39	50
Fire point (^{0}c)	48	56
TVOC Level (ppm)	0.38	0.37
Specific gravity	0.86	0.85
Smoke point	High	Very high

PDFO has a high smoke point, while Commercial Oil has a very high smoke point, indicating PDFO may produce smoke and break down at lower temperatures, making it less stable in high-heat environments. Despite this, PDFO's relatively high smoke point makes it suitable for applications where high-temperature stability is less critical, such as industrial heating processes, where its volatility and energy content are advantageous. The smoke point (SP), the maximum flame height before smoke formation [60], is influenced by aromatic content, with higher aromatic fuels producing more smoke and lower flame heights [61]. The higher SP of Commercial Oil suggests a lower tendency to produce soot, while PDFO's likely higher aromaticity may require refining to improve stability and performance.

Both oils exhibit similar Total Volatile Organic Compound (TVOC) levels – PDFO at 0.38 ppm and Commercial Oil at 0.37 ppm – indicating comparable contributions to air pollution. Their relatively low TVOC levels suggest suitability for use in environments requiring low VOC emissions, such as closed industrial systems or areas with strict environmental regulations. Notably, these values fall within the Occupational Safety and Health Administration's (OSHA) Permissible Exposure Level (PEL) of 0.75 ppm and action level of 0.5 ppm [62].

3.4. *Chemical characterisation of PDFOs*

3.4.1. *Effect of catalyst on hydrocarbon composition and distribution in pyrolytic oils*

The GCMS spectra (Fig. 7**)** show distinct differences in hydrocarbon composition across pyrolysis oils with and without a catalyst, and commercial oil. The catalysed PDFOs spectrum (**cf.** Fig. 7**A;** Table 2) is characterised by generally less pronounced hydrocarbon peaks, except for a dominant, highly pronounced peak at 30.45 min corresponding to Bis(2-ethylhexyl) phthalate ($C_{24}H_{38}O_4$). This suggests that while the catalyst may promote selective cracking, it may also favour the retention or concentration of certain thermally stable plasticisers in the final product.

In contrast, the uncatalysed PDFO shows a broader peak distribution with a higher proportion of peaks (cf., Fig. 7**B;** Table 2) corresponding to heavier hydrocarbons, including iodinated alkanes, with a dominant nitrogen-containing aromatic compound ($C_{19}H_{12}N_2O_3$) at 40.21 min, indicating less controlled thermal degradation and more complex by-products and fewer lighter onesThe commercial oil spectrum, typical of a refined product, shows a balanced distribution of peaks dominated by straight-chain alkanes, with the most intense peak corresponding to $C_{16}H_{34}$ **(cf.,** Fig. 7**C;** Table 2**)**.

The carbon range distribution (Fig. 8) suggests the influence of the catalyst on the cracking process and the subsequent hydrocarbon distribution. In the absence of a catalyst, PDFO produces fewer short-chain hydrocarbons (C_1-C_4) at 7.2 %, compared to 13.2 % with the catalyst and 9.7 % in commercial oil. This suggests that the catalyst enhances the breakdown of larger molecules into smaller ones, increasing the production of short-chain hydrocarbons. Similarly, in the presence of the

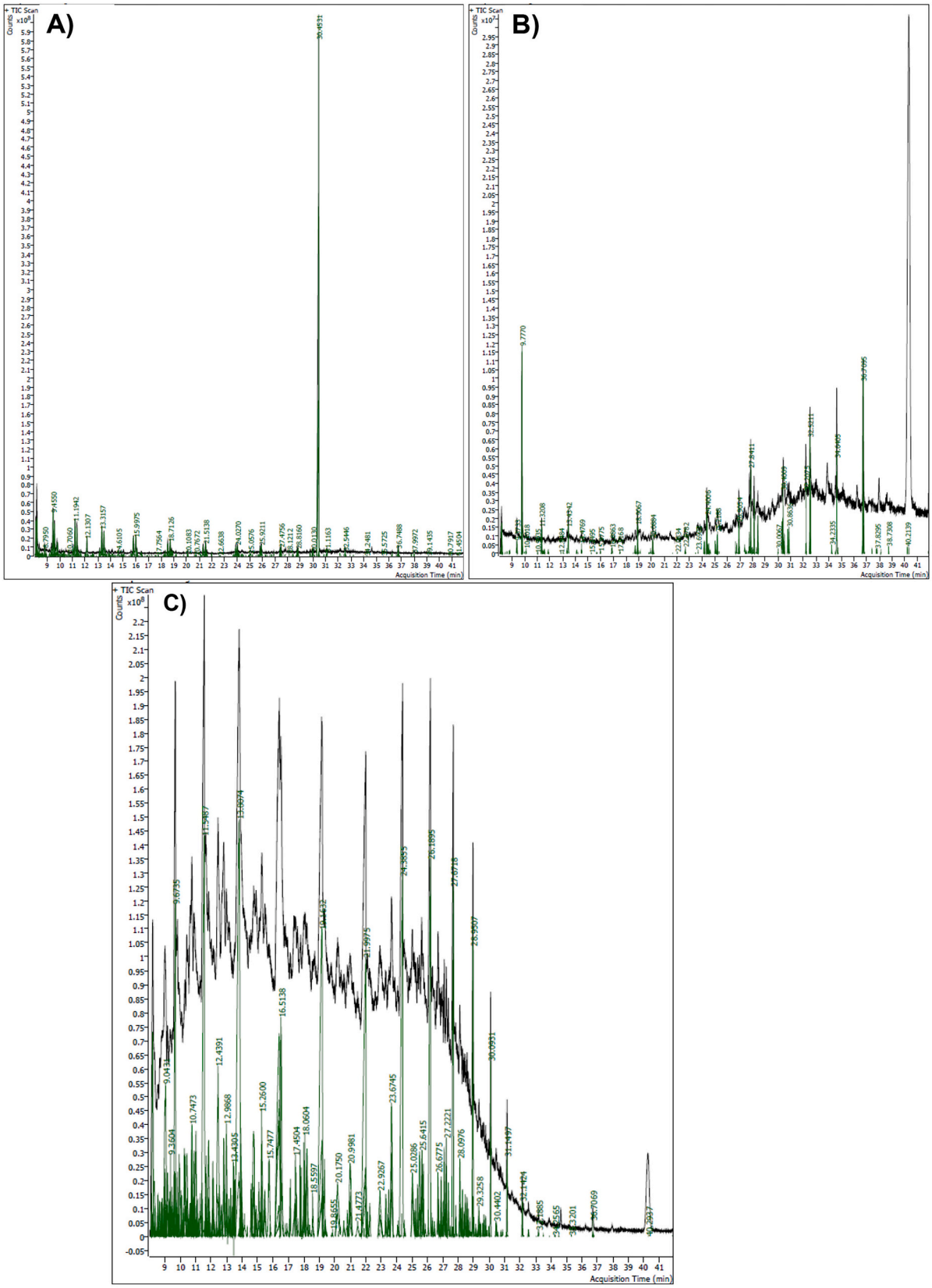


Fig. 7. The GC–MS spectra presented in Figs. A, B, and C correspond to the fuel types PDFO in the presence of a catalyst (**A**), PDFO in the absence of a catalyst **(B)**, and commercial oil (**C).**

Table 2
GC–MS spectral data showing the compounds corresponding to the dominant peaks for the different fuel types: PDFO (catalysed), PDFO (uncatalysed), and the commercial oils, and their respective retention times.

Fuel type	Retention time	Compound	Chemical formula
PDFO (catalysed)	9.45	Cyclodecane, methyl-	$C_{11}H_{22}$
	11.19	1-Tridecene	$C_{13}H_{26}$
	12.13	Benzophenone	$C_{13}H_{10}O$
	13.31	Oxalic acid, allyl hexadecyl ester	$C_{21}H_{38}O_4$
	18.71	1H- Tetrazol- 5-amine	CH_3N_5
	30.45 (most dominant)	Bis(2-ethyl(hexylphthalate)	$C_{24}H_{38}O_4$
PDFO (Uncatalysed)	9.77	2,4-Di-tert-butylphenol	$C_{14}H_{22}O$
	11.32	Sulfurous acid, 2-ethylhexyl hexyl ester	$C_{14}H_{30}O_3S$
	13.43	Tetradecane, 1-iodo-	$C_{14}H_{29}I$
	18.90	Dodecane, 1-iodo-	$C_{12}H_{25}I$
	27.84	Octacosane, 1- iodo	$C_{28}H_{57}I$
	30.40	Heptacosane	$C_{27}H_{56}$
	32.52	1,3-Benzene dicarboxylic acid, bis (2-ethylhyexyl)estet	$C_{24}H_{38}O_4$
	40.21(dominant)	Pyridine-3-carbonitrile, 1,2-dihydro-6-(1,3-benzodioxol-5-yl)-2-oxo-4-phenyl-	$C_{19}H_{12}N_2O_3$
Commercial Oil	9.66	Pentadecane	$C_{15}H_{32}$
	11.53 (dominant peak)	Hexadecane	$C_{16}H_{34}$
	13.78	Decane, 6-ethyl-2-methyl	$C_{13}H_{28}$
	16.38	Hexadecane	$C_{16}H_{34}$
	19.13	Nonane, 2-methyl-5-propyl	$C_{13}H_{28}$
	21.94	Hexadecane	$C_{16}H_{34}$
	24.33	Isolan	$C_{10}H_{17}N_3O_2$
	26.15	Heptocasone	$C_{27}H_{56}$
	31.15	Nonane, 2-methyl-5-propyl	$C_{13}H_{28}$

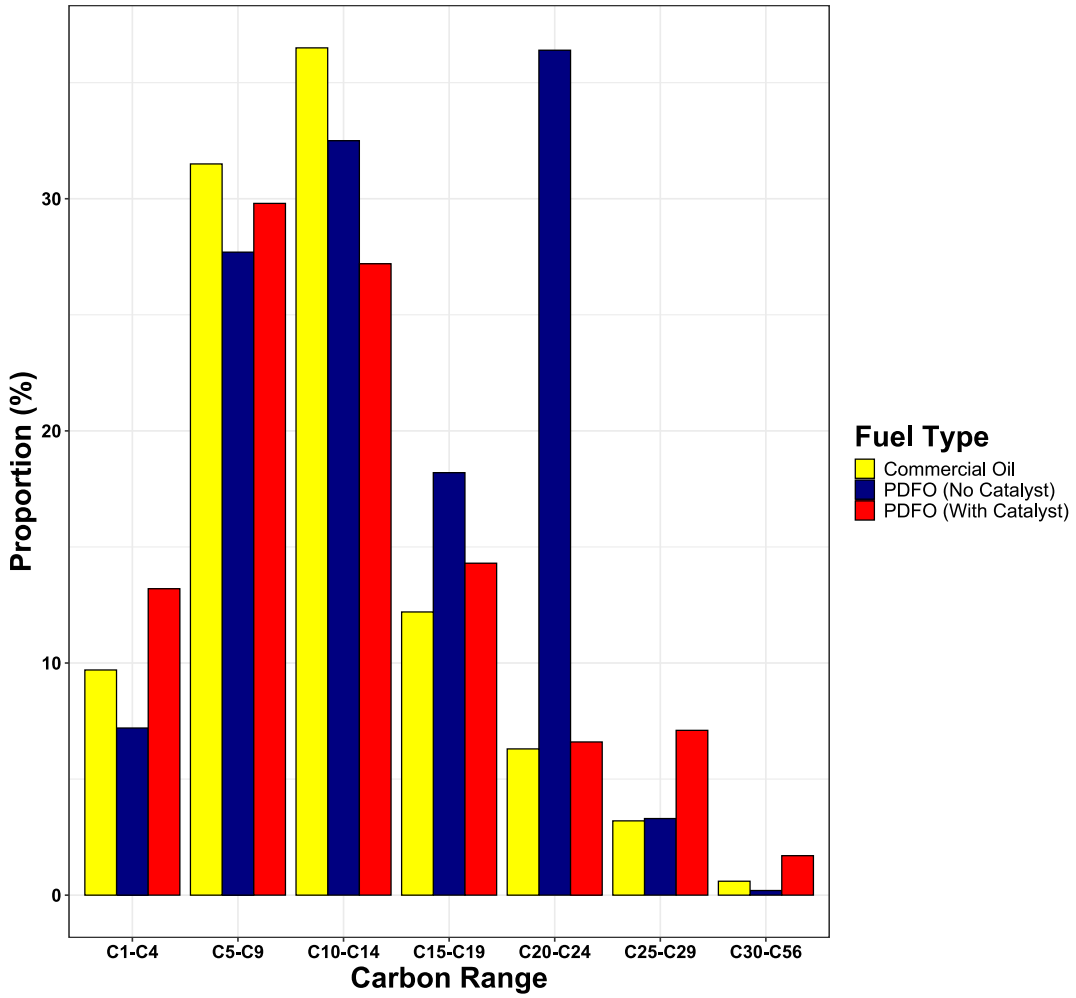


Fig. 8. Bar plot showing the proportions of carbon ranges in different fuel types: PDFO (No Catalyst), PDFO (With Catalyst), and Commercial Oil. The x-axis represents the carbon range categories, while the y-axis displays the proportion (%) of each category within the respective fuel type.

catalyst, the proportion of light hydrocarbons (C_5-C_9) increases, making the distribution closer to that of commercial oil. These findings align with the observations of Nisar et al. [63], who reported a broad range of hydrocarbons (C_4 to C_{21}) from catalytic pyrolysis using a cobalt-doped molecular sieve.

Similar to the previous studies [64,65,19], the middle chain hydrocarbons (C_{10}-C_{14} - diesel range; [66]) dominate the PDFOs. However, these are lower in the catalysed PDFOs (27.2 %) than in the commercial oils (36.5 %) and uncatalysed PDFOs (32.5 %). This suggests that the catalyst favours the further cracking of middle hydrocarbons into lighter fractions. In fact, in the case of heavy hydrocarbons (C_{15}-C_{19}), PDFO without a catalyst produces the highest proportion (18.2 %), while the catalyst reduces this to 14.3 %, closer to commercial oil at 12.2 %. A similar trend is observed for very heavy hydrocarbons (C_{20}-C_{24}), where the catalyst significantly reduces their proportion from 36.4 % (without a catalyst) to 6.6 %, aligning closely with commercial oil at 6.3 %.

However, the distribution of ultra-heavy hydrocarbons (C_{25}-C_{29} and C_{30}-C_{56}) shows a slight increase with the presence of a catalyst. For example, C_{25}-C_{29} hydrocarbons increased from 3.3 % (uncatalysed) to 7.1 % in the catalysed PDFO, compared to 3.2 % in commercial oil, while C_{30}-C_{56} hydrocarbons rose from 0.2 % in uncatalysed PDFO to 1.7 % in the catalysed PDFO, exceeding the 0.6 % observed in commercial oil. This observation suggests that whilst the catalyst effectively promotes cracking of heavy hydrocarbons into lighter fractions, it also results in the formation of small amounts of ultra-heavy hydrocarbons, potentially as a by-product of incomplete cracking. These ultra-heavy fractions, although present in low proportions, could negatively impact combustion efficiency.

3.4.2. *Catalytic mechanism of Nanopyroxene in plastic waste pyrolysis*

Nanopyroxene's catalytic efficacy in plastic waste pyrolysis is likely driven by its transition metal ions (e.g., Fe^{2+}/Fe^{3+}) embedded within its inosilicate structure, which enable redox reactions critical for polymer degradation [67]. During pyrolysis, these metal sites lower the activation energy for C—C and C—H bond scission, promoting cracking and dehydrogenation of plastic-derived intermediates into lighter hydrocarbons, thereby enhancing fuel yield and optimizing hydrocarbon distribution. The high surface area of nanopyroxene nanoparticles (20–50 nm) facilitates adsorption of polymeric fragments [67]. Although direct studies on nanopyroxene in pyrolysis were not mechanistically detailed in this study, its mechanism aligns with transition metal-based catalysts used in similar processes [46], suggesting that Fe-mediated redox cycles are central to its performance.

3.5. *Comparison of Nanopyroxene's potential with other catalytic additives*

The results of this study demonstrate that nanopyroxene significantly improves fuel yield in the mixed thermal pyrolysis of LDPE, PP, and HDPE, increasing the yield from 56 % without the catalyst to 77 % with it. This contrasts with Bagri & Williams [30], who reported a reduction in oil yield from 95 % (without catalyst) to 85 % with a Y-zeolite catalyst, highlighting differences in catalyst performance. Conversely, Saeaung et al.[33] found oil yields of 47 %–70 % from these plastics while using LTA zeolite catalysts, showing that nanopyroxene performs competitively, especially when compared to these zeolite catalysts.

Nanopyroxene also alters the chemical distribution of pyrolysis products, as discussed in **Section 3.4.1.** This mirrors Saeaung et al. [33]'s findings with LTA zeolite catalysts, which also revealed enhanced light hydrocarbons. However, nanopyroxene produced a slightly lower proportion of light hydrocarbons than zeolite catalysts. Whilst LTA zeolites increased gasoline-range hydrocarbons, nanopyroxene's distribution is closer to commercial oil used in this study, though LTA zeolite catalysts seem to outperform in light hydrocarbon production.

Nanopyroxene significantly reduces the fraction of heavy hydrocarbons (C_{20}–C_{24}), consistent with the catalytic cracking behaviour observed by Mikulec & Vrbova [68] using natural zeolites. Mikulec & Vrbova [68] suggested that zeolite catalysts promote the cracking of heavy hydrocarbons, which nanopyroxene also appears to do effectively. A notable difference in our findings is the slight increase in ultra-heavy hydrocarbons (C_{25}–C_{29} and C_{30}–C_{56}), from 3.3 % to 7.1 % and from 0.2 % to 1.7 %, respectively, when nanopyroxene is used. These values exceed those seen in commercial oil, which is quite unusual. Mikulec & Vrbova [68] did not observe such a trend with zeolites, suggesting that nanopyroxene may offer enhanced selectivity for heavier fractions. This behaviour could be advantageous for specific industrial applications, such as the production of heavy lubricants or fuel oils, though further investigation is needed to assess its implications for processing efficiency and catalyst stability.

When compared to other catalytic additives like Y-zeolite, ZSM-5, and silica-alumina, nanopyroxene demonstrates a balanced trade-off between yield and product distribution. Panda & Singh [69] reported that silica-alumina catalysts increased liquid yields up to 82.58 % in PP pyrolysis; however, nanopyroxene appears to offer better control over both light and heavy hydrocarbon fractions. While the differences in yield can be partly attributed to the difference in the feedstock, the observed reduction in very heavy hydrocarbons (C_{20}–C_{24}) and the controlled increase in ultra-heavy hydrocarbons (C_{25}–C_{29} and C_{30}–C_{56}) suggest that nanopyroxene provides more flexibility in tailoring the final product distribution. In contrast, zeolite catalysts typically favour lighter fractions.

Despite its relatively lower BET surface area (178.0 m^2/g), as reported in this study and corroborated by Hmoudah[48], nanopyroxene surpasses that of red mug clay (27.49 m^2/g), but remains significantly lower than ZSM-5 (412.0 m^2/g) as reported by López et al. [32]. This difference likely accounts for nanopyroxene's reduced efficiency in cracking and reforming large hydrocarbon molecules from high-molecular-weight polymers when compared to ZSM-5.

4. Conclusion

This study demonstrates that nanopyroxene-catalysed pyrolysis can significantly enhance oil yield and improve the hydrocarbon distribution towards lighter fractions, offering a potentially valuable waste-to-fuel pathway. Thermal catalytic pyrolysis of mixed waste plastics (LDPE, HDPE, PP) using nanopyroxene produced char, condensable, and non-condensable gases, with a maximum oil yield of 77 % (catalysed) versus 56 % (non-catalysed). Extending the holding time by incremental 20 min, increased fuel yield until stabilisation, with the catalyst enhancing light hydrocarbon (C_1–C_9) production and reducing middle (C_{10}–C_{14}) and heavy hydrocarbons (C_{15}–C_{24}). Despite improving the hydrocarbon profile to resemble commercial oil, catalysis increased ultra-heavy hydrocarbons (C_{25}–C_{56}), potentially affecting combustion efficiency.

PDFOs exhibited higher volatility, density, and flammability than commercial oil, with a lower flashpoint (39 °C) and fire point (48 °C), making it ideal for niche applications requiring high combustion energy, while commercial oil remains preferable for conventional, stable applications. PDFO's high smoke point and similar volatile organic compound (VOC) levels to commercial oil indicate usability in low-VOC environments.

A detailed sustainability assessment is recommended to evaluate the environmental, economic, and social impacts of this catalytic pyrolysis approach in practical waste management scenarios.

5. Strengths, limitations and future prospects

5.1. *Strengths*

This study presents a novel application of nanopyroxene as a catalytic additive in the pyrolysis of plastic waste, contributing new knowledge to the development of alternative catalysts for sustainable

fuel production. The use of a locally designed thermal pyrolysis reactor demonstrates practical relevance and potential scalability, particularly for low-income regions facing pressing plastic pollution and energy scarcity. By focusing on the most abundant environmental plastics (LDPE, HDPE, and PP), the findings are broadly applicable to typical real-world waste streams.

5.2. Limitations and future work

In this study, the polymer-to-catalyst ratio was fixed at 10:1, based on prior literature, and was not varied, which limits understanding of how catalyst loading affects product yield and quality. Similarly, operational parameters such as temperature and reaction time were also held constant, restricting further optimisation specific to nanopyroxene's catalytic behaviour under different reaction conditions. The detailed characterisations of gaseous and solid by-products extended beyond the scope of this manuscript. A comprehensive mass and energy balance, including calorific value determination of the fuel oils and quantification of all by-products, was not performed. While char and non-condensable gases were qualitatively observed during pyrolysis, detailed chemical characterisation and yield estimation of these by-products extended beyond the scope of this work. Furthermore, the experiments were conducted at laboratory scale, and potential challenges related to scale-up and catalyst longevity remain unexplored. Emissions and broader environmental consequences of catalytic pyrolysis process are essential areas for future assessments. Additionally, Future studies should explore catalyst modification or post-treatment strategies to further improve the fuel purity and reduce the presence of plasticiser-related compounds.

CRediT authorship contribution statement

Derick Muloogi: Writing – original draft, Visualization, Software, Resources, Project administration, Methodology, Investigation, Funding acquisition, Formal analysis, Data curation, Conceptualization. **Farad Sagala:** Writing – review & editing, Resources, Methodology, Investigation, Funding acquisition, Conceptualization. **Fortunate Ogene:** Writing – review & editing, Software, Data curation. **Denis Bbosa:** Writing – review & editing, Investigation. **Grace Birungi:** Writing – review & editing, Supervision.

Declaration of competing interest

The authors declare that they have no known competing financial interests or personal relationships that could have appeared to influence the work reported in this paper.

Acknowledgements

The authors thank the Government of Uganda, through the Directorate of Research and Graduate Training (DRGT) at Mbarara University of Science and Technology, for providing financial support for this research (to DM et al 2022–2023). This project also received seed grant funding from the Centre for Innovation and Technology Transfer (CITT) at Mbarara University of Science and Technology (to DM et al 2021–2022). We further acknowledge the contributions of our research assistants – Anxious Tumukunde, Macholi Chris Benard, Kirabo Claire, Najuna Muganzi, Opok Haron Otim, Pauline Kumanya, Atukunda Sharon, and Kiiza Victor – whose efforts were invaluable in the successful completion of this project. We also thank Benedicto Bukyana at the Faculty of Applied Sciences and Technology (FAST) laboratories and Stanley Kizito at the Government Analytical Laboratory in Wandegeya for the analytical support. Special appreciation is extended to the Dr. Nassar's Nanotechnology Research Group at the University of Calgary whose previous works have inspired this research. We thank the two anonymous reviewers for their comments which have significantly improved the clarity of the manuscript. The views expressed here do not necessarily represent those of the institutions, funders, or individuals whose support is acknowledged.

Data availability

All supplementary data, including comprehensive spectral information, can be accessed on request from the corresponding author.

References

[1] J. Hopewell, R. Dvorak, E. Kosior, Plastics recycling: challenges and opportunities, Philos. Trans. R. Soc., B 364 (1526) (2009) 2115–2126.
[2] O. Olatunji, Re-Envisioning Plastics Role in the Global Society: Perspectives on Food, Urbanization, and Environment, Springer Nature, 2024.
[3] D.V. Rosato, Plastics End Use Applications, Springer Science & Business Media, 2011.
[4] N. Ferronato, V. Torretta, Waste mismanagement in developing countries: a review of global issues, Int. J. Environ. Res. Public Health 16 (6) (2019), https://doi.org/10.3390/ijerph16061060.
[5] D. Muloogi, C. Ruhabwa, M. Ampiire, R. Arinwamukama, Assessment of selected Physico-chemical properties of leachate at Kenkombe dumping site, Mbarara City and modelling of surface water quality of Rwentondo stream, European Journal of Science, Innovation and Technology 1 (6) (2021) 1–11.
[6] T.I.S. Swati, V.K. Vijay, P. Ghosh, Scenario of landfilling in India: problems, challenges, and recommendations, Handbook of Environmental Materials Management 10 (2018) 973–978.
[7] N. Yang, H. Zhang, M. Chen, L.-M. Shao, P.-J. He, Greenhouse gas emissions from MSW incineration in China: impacts of waste characteristics and energy recovery, Waste Manag. 32 (12) (2012) 2552–2560, https://doi.org/10.1016/j.wasman.2012.06.008.
[8] D.K.A. Barnes, F. Galgani, R.C. Thompson, M. Barlaz, Accumulation and fragmentation of plastic debris in global environments, Philosophical Transactions of the Royal Society B: Biological Sciences 364 (1526) (2009) 1985–1998, https://doi.org/10.1098/rstb.2008.0205.
[9] W. d'Ambrières, Plastics recycling worldwide: current overview and desirable changes. *Field actions science reports*, The Journal of Field Actions, Special Issue 19 (2019) 12–21.
[10] T. Hundertmark, M. Mayer, C. McNally, T.J. Simons, C. Witte, How plastics waste recycling could transform the chemical industry, McKinsey & Company 12 (2018) 1.
[11] C.M. Wandeka, N. Kiggundu, R. Mutumba, Plastic Packaging: A Study on Plastic Imports in Uganda, 2022.
[12] A. Ozoh, B. Longe, V. Akpe, I. Cock, Indiscriminate solid waste disposal and problems with water-polluted urban cities in Africa, Journal of Coastal Zone Management 24 (S5) (2021) 1000005.
[13] S.K. Tulashie, E.K. Boadu, F. Kotoka, D. Mensah, Plastic wastes to pavement blocks: a significant alternative way to reducing plastic wastes generation and accumulation in Ghana, Construct. Build Mater. 241 (2020) 118044, https://doi.org/10.1016/j.conbuildmat.2020.118044.
[14] K. Ragaert, L. Delva, K. Van Geem, Mechanical and chemical recycling of solid plastic waste, Waste Manag. 69 (2017) 24–58.
[15] Q. Zhang, J. Chen, X. Guo, H. Lei, R. Zou, E. Huo, X. Kong, W. Liu, M. Wang, Z. Ma, Mussel-inspired polydopamine-modified biochar microsphere for reinforcing polylactic acid composite films: emphasizing the achievement of excellent thermal and mechanical properties, Int. J. Biol. Macromol. 260 (2024) 129567.
[16] Q. Zhang, D. Zhang, H. Xu, W. Lu, X. Ren, H. Cai, H. Lei, E. Huo, Y. Zhao, M. Qian, Biochar filled high-density polyethylene composites with excellent properties: towards maximizing the utilization of agricultural wastes, Ind. Crop. Prod. 146 (2020) 112185.
[17] V. Mangesh, S. Padmanabhan, P. Tamizhdurai, A. Ramesh, Experimental investigation to identify the type of waste plastic pyrolysis oil suitable for conversion to diesel engine fuel, J. Clean. Prod. 246 (2020) 119066.
[18] S. Padmanabhan, K. Giridharan, B. Stalin, S. Kumaran, V. Kavimani, N. Nagaprasad, L. Tesfaye Jule, R. Krishnaraj, Energy recovery of waste plastics into diesel fuel with ethanol and ethoxy ethyl acetate additives on circular economy strategy, Sci. Rep. 12 (1) (2022) 5330.
[19] B.K. Sharma, B.R. Moser, K.E. Vermillion, K.M. Doll, N. Rajagopalan, Production, characterization and fuel properties of alternative diesel fuel from pyrolysis of waste plastic grocery bags, Fuel Process. Technol. 122 (2014) 79–90.
[20] S. Al-Salem, A. Antelava, A. Constantinou, G. Manos, A. Dutta, A review on thermal and catalytic pyrolysis of plastic solid waste (PSW), J. Environ. Manage. 197 (2017) 177–198.
[21] A. Demirbas, B.O. Al-Sasi, A.-S. Nizami, Conversion of waste tires to liquid products via sodium carbonate catalytic pyrolysis, Energy Sources, Part A 38 (16) (2016) 2487–2493.
[22] P.A. Owusu, N. Banadda, A. Zziwa, J. Seay, N. Kiggundu, Reverse engineering of plastic waste into useful fuel products, J. Anal. Appl. Pyrolysis 130 (2018) 285–293.
[23] S. Kumar, R.K. Singh, Recovery of hydrocarbon liquid from waste high density polyethylene by thermal pyrolysis. In, Braz. J. Chem. Eng. 28 (2011) scielo.

[24] R. Miandad, M.A. Barakat, A.S. Aburiazaiza, M. Rehan, A.S. Nizami, Catalytic pyrolysis of plastic waste: a review, Process Saf. Environ. Prot. 102 (2016) 822–838, https://doi.org/10.1016/j.psep.2016.06.022.
[25] A.G. Batte, A. Muwanga, P.W. Sigrist, M. Owor, Vertical electrical sounding as an exploration technique to improve on the certainty of groundwater yield in the fractured crystalline basement aquifers of eastern Uganda, Hydrgeol. J. 16 (8) (2008) 1683–1693, https://doi.org/10.1007/s10040-008-0348-4.
[26] C.J. Wrasman, A.N. Wilson, O.D. Mante, K. Iisa, A. Dutta, M.S. Talmadge, D. C. Dayton, S. Uppili, M.J. Watson, X. Xu, Catalytic pyrolysis as a platform technology for supporting the circular carbon economy, Nat. Catal. 6 (7) (2023) 563–573.
[27] V. Mangesh, T. Perumal, S. Subramanian, S. Padmanabhan, Clean energy from plastic: production of hydroprocessed waste polypropylene pyrolysis oil utilizing a Ni–Mo/laponite catalyst, Energy Fuel 34 (7) (2020) 8824–8836.
[28] D. Achilias, C. Roupakias, P. Megalokonomos, A. Lappas, E. Antonakou, Chemical recycling of plastic wastes made from polyethylene (LDPE and HDPE) and polypropylene (PP), J. Hazard. Mater. 149 (3) (2007) 536–542.
[29] F.J. Passamonti, U. Sedran, Recycling of waste plastics into fuels. LDPE conversion in FCC, Appl. Catal. Environ. 125 (2012) 499–506.
[30] R. Bagri, P.T. Williams, Catalytic pyrolysis of polyethylene, J. Anal. Appl. Pyrolysis 63 (1) (2002) 29–41.
[31] E. Erawati, H. Hamid, A.A. Ilma, Pyrolysis process of mixed polypropylene (PP) and high-density polyethylene (HDPE) waste with natural zeolite as catalyst, Molekul 13 (2) (2018) 106–113.
[32] A. López, I. de Marco, B.M. Caballero, M.F. Laresgoiti, A. Adrados, A. Aranzabal, Catalytic pyrolysis of plastic wastes with two different types of catalysts: ZSM-5 zeolite and red mud, Appl. Catal. Environ. 104 (3) (2011) 211–219, https://doi.org/10.1016/j.apcatb.2011.03.030.
[33] K. Saeaung, N. Phusunti, W. Phetwarotai, S. Assabumrungrat, B. Cheirsilp, Catalytic pyrolysis of petroleum-based and biodegradable plastic waste to obtain high-value chemicals, Waste Manag. 127 (2021) 101–111.
[34] B. Thangaraj, Y.-K. Lee, Review on recent development in catalytic cracking of waste polyolefins: effect of zeolite-based catalysts and reaction parameters, Fuel 380 (2025) 133220.
[35] Z. Demrew Yigezu, K. Muthukumar, Structural characteristics of selected metal oxides used for the catalytic pyrolysis of sunflower oil, J. Anal. Appl. Pyrolysis 114 (2015) 60–67, https://doi.org/10.1016/j.jaap.2015.05.002.
[36] Q. Li, L.-S. Wang, B.-Y. Hu, C. Yang, L. Zhou, L. Zhang, Preparation and characterization of NiO nanoparticles through calcination of malate gel, Mater. Lett. 61 (8) (2007) 1615–1618, https://doi.org/10.1016/j.matlet.2006.07.113.
[37] Y. Ishihara, H. Nanbu, T, Ikemura and T, Takesue. *Fuel* 69 (1990) 978.
[38] S.R. Ivanova, E.F. Gumerova, Aleksandr A. Berlin, Karl S. Minsker, Gennadii E. Zaikov, Catalytic degradation of polyolefins—a promising method for the regeneration of monomers, Russ. Chem. Rev. 60 (2) (1991) 225, https://doi.org/10.1070/RC1991v060n02ABEH001041.
[39] Y. Uemichi, K. Takuma, A. Ayame, Chemical recycling of poly (ethylene) by catalytic degradation into aromatic hydrocarbons using H-ga-silicate, Chem. Commun. 18 (1998) 1975–1976.
[40] A. Corma, State of the art and future challenges of zeolites as catalysts, J. Catal. 216 (1–2) (2003) 298–312.
[41] O. Norouzi, S. Taghavi, P. Arku, S. Jafarian, M. Signoretto, A. Dutta, What is the best catalyst for biomass pyrolysis? J. Anal. Appl. Pyrolysis 158 (2021) 105280.
[42] A. Pattiya, Catalytic pyrolysis, Direct Thermochemical Liquefaction for Energy Applications (2018) 29–64, https://doi.org/10.1016/B978-0-08-101029-7.00002-3.
[43] Y.-H. Seo, K.-H. Lee, D.-H. Shin, Investigation of catalytic degradation of high-density polyethylene by hydrocarbon group type analysis, J. Anal. Appl. Pyrolysis 70 (2) (2003) 383–398.
[44] J. Leng, Z. Wang, J. Wang, H.-H. Wu, G. Yan, X. Li, H. Guo, Y. Liu, Q. Zhang, Z. Guo, Advances in nanostructures fabricated via spray pyrolysis and their applications in energy storage and conversion, Chem. Soc. Rev. 48 (11) (2019) 3015–3072.
[45] B. Hvolbæk, T.V.W. Janssens, B.S. Clausen, H. Falsig, C.H. Christensen, J. K. Nørskov, Catalytic activity of au nanoparticles, Nano Today 2 (4) (2007) 14–18.
[46] F. Sagala, T. Montoya, A. Hethnawi, G. Vitale, N.N. Nassar, Nanopyroxene-based nanofluids for enhanced oil recovery in sandstone cores at reservoir temperature, Energy Fuel 33 (2) (2019) 877–890.
[47] G. Vitale, Iron Silicate Nano-Crystals as Potential Catalysts or Adsorbents for Heavy Hydrocarbons Upgrading, University of Calgary, 2013.
[48] M.B. Hmoudah, Nano-Pyroxene for Adsorption and Catalytic Thermal Decomposition of Visbroken Residue Asphaltenes, University of Calgary (Canada), 2016.
[49] A. Hethnawi, N.N. Nassar, A.D. Manasrah, G. Vitale, Polyethylenimine-functionalized pyroxene nanoparticles embedded on diatomite for adsorptive removal of dye from textile wastewater in a fixed-bed column, Chem. Eng. J. 320 (2017) 389–404.
[50] F. Sagala, A. Hethnawi, N.N. Nassar, Hydroxyl-functionalized silicate-based nanofluids for enhanced oil recovery, Fuel 269 (2020) 117462.
[51] P. Echlin, Handbook of Sample Preparation for Scanning electron Microscopy and X-Ray Microanalysis, Springer Science & Business Media, 2011.
[52] C.A. Joshi, J.R. Seay, An appropriate technology based solution to convert waste plastic into fuel oil in underdeveloped regions, Journal of Sustainable Development 9 (4) (2016) 133–143.
[53] C.J. Jangid, K.M. Miller, J.R. Seay, Analysis of Plastic-Derived Fuel Oil Produced from High- and Low-Density Polyethylene, 2022.
[54] ASTM, Standard Test Method for Density, Relative Density, or API Gravity of Crude Petroleum and Liquid Petroleum Products by Hydrometer Method, ASTM International West Conshohocken, PA, USA, 2017.
[55] X. Zhang, L. Pan, L. Wang, J.-J. Zou, Review on synthesis and properties of high-energy-density liquid fuels: hydrocarbons, nanofluids and energetic ionic liquids, Chem. Eng. Sci. 180 (2018) 95–125.
[56] A. Angyal, N. Miskolczi, L. Bartha, Petrochemical feedstock by thermal cracking of plastic waste, J. Anal. Appl. Pyrolysis 79 (1–2) (2007) 409–414.
[57] D. Olsen, E.B. Ramzel, Heavy oil refining and transportation: effect on the feasibility of increasing domestic heavy oil production, Fuel 71 (12) (1992) 1391–1401.
[58] M.Z.H. Khan, M. Sultana, M.R. Al-Mamun, M.R. Hasan, Pyrolytic waste plastic oil and its diesel blend: fuel characterization, J. Environ. Public Health 2016 (2016), https://doi.org/10.1155/2016/7869080.
[59] CEN. (2009). *EN 590:2009 – automotive fuels – diesel – requirements and test methods*.
[60] M.A.A. Qasem, E.M. Al-Mutairi, A.G.A. Jameel, Smoke point prediction of oxygenated fuels using neural networks, Fuel 332 (2023) 126026.
[61] N. Ladommatos, Z. Xiao, H. Zhao, Effects of fuels with a low aromatic content on diesel engine exhaust emissions, Proceedings of the Institution of Mechanical Engineers, Part D: Journal of Automobile Engineering 214 (7) (2000) 779–794.
[62] A.H. Mitchell, A.H. Mitchell, Occupational safety and health administration (OSHA) regulatory compliance, Preventing Occupational Exposures to Infectious Disease in Health Care: A Practical Guide (2020) 51–66.
[63] J. Nisar, M.A. Khan, G. Ali, A. Shah, M. Iqbal, I.A. Bhatti, Cobalt-doped molecular sieve for efficient degradation of polypropylene into fuel oil: kinetics and fuel properties of the oil, Chem. Eng. Res. Des. 177 (2022) 751–758, https://doi.org/10.1016/j.cherd.2021.11.038.
[64] C. Kaewbuddee, E. Sukjit, J. Srisertpol, S. Maithomklang, K. Wathakit, N. Klinkaew, P. Liplap, W. Arjharn, Evaluation of waste plastic oil-biodiesel blends as alternative fuels for diesel engines, Energies 13 (11) (2020) 2823.
[65] V. Mangesh, S. Padmanabhan, S. Ganesan, D. PrabhudevRahul, T.D.K. Reddy, Prospects of pyrolysis oil from plastic waste as fuel for diesel engines: A review. 197 (1) (2017) 012027.
[66] S. Kuppusamy, N.R. Maddela, M. Megharaj, K. Venkateswarlu, S. Kuppusamy, N. R. Maddela, M. Megharaj, K. Venkateswarlu, An Overview of Total Petroleum Hydrocarbons, Environmental Fate, Toxicity, and Remediation, Total Petroleum Hydrocarbons, 2020, pp. 1–27.
[67] G. Nafie, G. Vitale, L. Carbognani Ortega, N.N. Nassar, Nanopyroxene grafting with β-cyclodextrin monomer for wastewater applications, ACS Appl. Mater. Interfaces 9 (48) (2017) 42393–42407.
[68] J. Mikulec, M. Vrbova, Catalytic and thermal cracking of selected polyolefins, Clean Techn. Environ. Policy 10 (2) (2008) 121–130.
[69] A.K. Panda, R. Singh, Catalytic performances of kaoline and silica alumina in the thermal degradation of polypropylene, J. Fuel Chem. Technol. 39 (3) (2011) 198–202.